

Analytical solution on MHD Non-Newtonian fluid (Walter's B-Model) flow past an infinite vertical plate through porous medium

Vasa Raghu¹, G S S Raju², A G Vijaya Kumar³

¹Research Scholar (PP.MAT.0138), Department of Mathematics, Rayalaseema University, Kurnool, AP, INDIA

²Department of Mathematics, JNT college of Engineering, Pulivendula, AP, INDIA

³Department of Mathematics, SAS, VIT, Vellore, INDIA

Abstract- An investigation has been carried out to analysis an unsteady free convective chemically reacting, MHD Non-Newtonian fluid (Walter's liquid-B model) flow past an infinite vertical plate with uniform temperature and concentration in the presence of transverse magnetic field through porous medium. The dimensionless governing partial differential equations are solved using Laplace transform technique. They satisfy all imposed initial and boundary conditions and for $S \rightarrow 0$ can be reduced to the similar solutions for Newtonian fluids. The solution of velocity, temperature and concentration as well as the rate of heat and mass transfer characteristics are analyzed by plotting graphs, the physical aspects are discussed in detail to interpret the effect of significant parameters like magnetic field, porous medium, thermal Grashof number, mass Grashof number, radiation parameter, Prandtl number, Schmidt number and first order chemical reaction of the problem.

Keywords – Porous medium, chemical reaction, MHD, Non-Newtonian fluid, free convection, heat and mass transfer.

I. INTRODUCTION

The flow of an incompressible viscous fluid past impulsively started, infinite horizontal flat plate, in its own plane was first studied by Stokes [1]. Walters [2-3] formulated a system of constitutive equations for elasto-viscous fluid and of them is known as Walter's liquid 'B'. Kubair and Pei [4] studied theoretical analysis for the combined laminar free and forced convection heat transfer to non-Newtonian fluids in external flows. The impulsive motion of a flat plate in a viscoelastic fluid is studied by Teipel [5]. Bestman [6-7] studied laminar convection of a steady and unsteady radiating non-Newtonian fluid in a vertical porous channel. Singh [8] presented MHD free-convection flow past an uniformly accelerated vertical porous plate. In this study he took into consideration of both cooling and heating cases. Singh [9] studied the problem of MHD flow of an elastic-viscous fluid past an impulsively started vertical plate. Dandpath and Gupta [10] presented the flow and heat transfer in a visco-elastic fluid over a stretching shell. Only few authors studied viscoelastic fluid flow by using Laplace transform technique namely Choubey and Yadav [11], Jha [12], Samria [13], Chowdhury and Islam [14], Vijaya kumar et al. [15] and Kumaresan et al. [16]. Khan and Pop [17] studied unsteady free convective viscoelastic boundary layer flow past a vertical porous plate with internal heat generation/absorption was studied analytically. Hameed and Nadeem [18] investigated unsteady MHD flow of a non-Newtonian fluid on a porous plate. Damseh and Shannak [19] studied the viscoelastic fluid flow past an infinite vertical porous plate in the presence of first-order chemical reaction by using finite difference method. Numerical study of viscous dissipation effects on free convection heat and mass transfer of MHD non-Newtonian fluid flow through a porous medium have been discussed by Eldabe et al. [20]. Motivated by the above cited work, in this paper, we present an analytical solution on MHD Non-Newtonian fluid (Walter's B-Model) flow past an infinite vertical plate through porous medium with uniform temperature and concentration in the presence of transverse applied magnetic field. The dimensionless governing equations are solved using Laplace transform technique. The solutions are expressed in terms of exponential and complementary error functions. Exact solutions, on the other hand are needed not only for the technical relevance of the flows but are also significant for a variety of other reasons such as they can be used as a benchmark for numerical solvers and for checking the stability of their solutions.

II. PROBLEM DISCRPTION

2.1 Mathematical Analysis

The unsteady free convection and mass transfer flow of an electrically conducting incompressible visco-elastic fluid past an infinite vertical plate through porous medium in the presence of radiation and chemical reaction has been

considered. A transverse magnetic field of uniform strength B_0 is applied normal to the direction of the flow. The induced magnetic field is neglected in comparison to the applied magnetic field as the magnetic Reynolds number of the flow is taken to be very small. The flow is assumed to be in x' - direction which is taken along the vertical plate in upward direction against to the gravitational field and the y' - axis is taken to be normal to the plate. Initially the plate and the surrounding fluid are at the same temperature T_∞' with concentration level C_∞' at all points in stationary condition. At time $t > 0$, the plate is given an impulsive motion with a uniform velocity $U = U_0$ in its own plane and the plate temperature raised to T_w' and at the same time concentration is also raised to C_w' . For free convection flow, it is also assumed that

The viscous dissipation is neglected in the energy equation.

The effects of variation in density (ρ) with temperature and species concentration are considered only on the body force term, in accordance with usual Boussinesq's approximation.

The fluid considered here is gray, absorbing / eliminating radiation but a non-scattering medium.

The flow of the fluid is assumed to be in the direction of x' axis, so the physical quantities are functions of the coordinates y' and t' only.

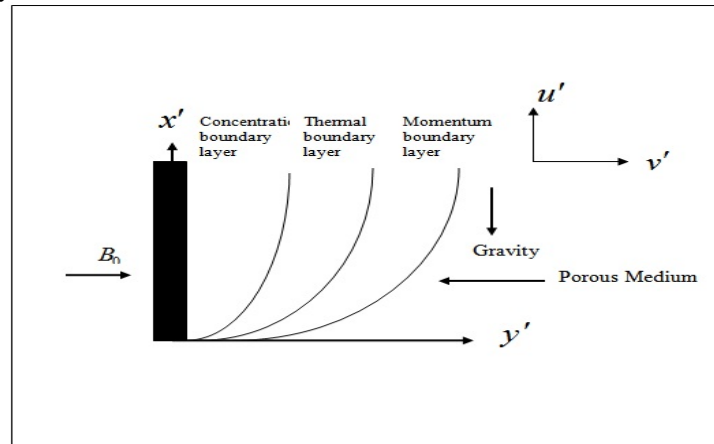


Figure 1 Physical model and co-ordinate system

By usual Boussinesq's approximation, the unsteady viscoelastic fluid flow is governed by the following equations

$$\frac{\partial u'}{\partial t'} = \nu \frac{\partial^2 u'}{\partial y'^2} - \frac{K_0}{\rho} \frac{\partial^3 u'}{\partial y'^2 \partial t'} - \frac{\sigma B_0^2 u'}{\rho} - \frac{\nu u'}{K'} + g\beta(T' - T_\infty') + g\beta^*(C' - C_\infty') \quad (1)$$

$$\rho C_p \frac{\partial T'}{\partial t'} = \kappa \frac{\partial^2 T'}{\partial y'^2} - \frac{\partial q_r}{\partial y'} \quad (2)$$

$$\frac{\partial C'}{\partial t'} = D \frac{\partial^2 C'}{\partial y'^2} - K_r (C' - C_\infty') \quad (3)$$

With the initial boundary conditions

$$\begin{aligned} t' \leq 0: \quad u' &= 0, \quad T' = T_\infty', \quad C' = C_\infty' && \text{for all } y' \\ t' > 0: \quad u' &= u_0, \quad T' = T_w', \quad C' = C_w' && \text{at } y' = 0 \\ u' &= 0, \quad T' \rightarrow T_\infty', \quad C' \rightarrow C_\infty' && \text{as } y' \rightarrow \infty \end{aligned} \quad (4)$$

$$A = \frac{u_0^2}{\nu}$$

Where ν . The local radiant for the case of an optically thin gray gas is expressed by $\frac{\partial q_r}{\partial y'} = -4a^* \sigma (T_\infty' - T'^4)$ (5)

It is assumed that the temperature differences within the flow are sufficiently small and that T'^4 may be expressed as a linear function of the temperature. This is obtained by expanding T'^4 in a Taylor series about T_∞' and neglecting the higher order terms, thus, we get $T'^4 \cong 4T_\infty'^3 T' - 3T_\infty'^4$ (6)

From equations (5) and (6), equation (2) reduces to

$$\rho C_p \frac{\partial T'}{\partial t'} = \kappa \frac{\partial^2 T'}{\partial y'^2} + 16a^* \sigma T_\infty'^3 (T_\infty' - T')$$
 (7)

On introducing the following non-dimensional quantities:

$$u = \frac{u'}{u_0}, t = \frac{t'u_0^2}{\nu}, y = \frac{y'u_0}{\nu}, \theta = \frac{T' - T_\infty'}{T_w' - T_\infty'}, C = \frac{C' - C_\infty'}{C_w' - C_\infty'}, G_r = \frac{g\beta\nu(T_w' - T_\infty')}{u_0^3}, Pr = \frac{\mu C_p}{\kappa}, M = \frac{\sigma B_0^2 \nu}{\rho u_0^2}$$

$$G_m = \frac{g\beta^* \nu (C_w' - C_\infty')}{u_0^3}, K = \frac{u_0^2 K'}{\nu^2}, a = \frac{a'\nu}{u_0^2}, k = \frac{\nu K_r}{u_0^2}, R = \frac{16a^* \nu^2 \sigma T_\infty'^3}{\kappa u_0^2}, S = \frac{K_0^2 u_0^2}{\rho \nu^2}, Sc = \frac{\nu}{D}$$
 (8)

Equations (1) to (4), lead to

$$\frac{\partial u}{\partial t} = \frac{\partial^2 u}{\partial y^2} - S \frac{\partial^3 u}{\partial y^2 \partial t} - Mu - \frac{u}{K} + G_r \theta + G_m C$$
 (9)

$$\frac{\partial \theta}{\partial t} = \frac{1}{Pr} \frac{\partial^2 \theta}{\partial y^2} - \frac{R}{Pr} \theta$$
 (10)

$$\frac{\partial C}{\partial t} = \frac{1}{Sc} \frac{\partial^2 C}{\partial y^2} - kC$$
 (11)

with the initial and boundary conditions:

$$t \leq 0; \quad u = 0, \quad \theta = 0, \quad C = 0 \quad \text{for all } y$$

$$t > 0; \quad u = 1, \quad \theta = 1, \quad C = 1 \quad \text{at } y = 0$$

$$u \rightarrow 0, \quad \theta \rightarrow 0, \quad C \rightarrow 0 \quad \text{as } y \rightarrow \infty$$
 (12)

All the physical parameters are defined in the nomenclature. For solving the problem, we take Beard and Walters [3]

U in the form $U = U_0 + SU_1$. The solution of equations (9) to (11) under initial and boundary conditions (9) and by the use of equation (12) and Laplace Transform Technique is thus given by:

$$U = B_1 + \frac{G_r}{R-P} [B_1 + B_5 - B_2 - B_4] + \frac{G_m}{kSc-P} [B_1 + B_7 - B_3 - B_6] + \frac{SG_r R}{(Pr-1)^2} [\exp(-bt)(B_8 - B_{10})]$$

$$+ \frac{SG_r Pr}{(Pr-1)^2} [b \exp(-bt)(B_{10} - B_8) + (B_2 - B_5)] + \frac{SG_m kSc}{(Sc-1)^2} [\exp(-ct)(B_9 - B_{11})]$$

$$\begin{aligned}
 & + \frac{SG_m Sc}{(Sc-1)^2} \left[c \exp(-ct)(B_{11} - B_9) + (B_3 - B_7) \right] - \frac{Sy}{2} [B_{12}] - \frac{SG_r y}{2(Pr-1)} [B_{13} + B_{14}] \\
 & - \frac{SG_m y}{2(Sc-1)} [B_{13} + B_{15}]
 \end{aligned} \tag{13}$$

$$\theta = \frac{1}{2} \left[\exp(y\sqrt{R}) \operatorname{erfc} \left(\frac{y\sqrt{Pr}}{2\sqrt{t}} + \sqrt{\frac{Rt}{Pr}} \right) + \exp(-y\sqrt{R}) \operatorname{erfc} \left(\frac{y\sqrt{Pr}}{2\sqrt{t}} - \sqrt{\frac{Rt}{Pr}} \right) \right] \tag{14}$$

$$C = \frac{1}{2} \left[\exp(y\sqrt{kSc}) \operatorname{erfc} \left(\frac{y\sqrt{Sc}}{2\sqrt{t}} + \sqrt{kt} \right) + \exp(-y\sqrt{kSc}) \operatorname{erfc} \left(\frac{y\sqrt{Sc}}{2\sqrt{t}} - \sqrt{kt} \right) \right] \tag{15}$$

where

$$B_1 = \frac{1}{2} \left[\exp(y\sqrt{P}) \operatorname{erfc} \left(\frac{y}{2\sqrt{t}} + \sqrt{Pt} \right) + \exp(-y\sqrt{P}) \operatorname{erfc} \left(\frac{y}{2\sqrt{t}} - \sqrt{Pt} \right) \right]$$

$$B_2 = \frac{\exp(-bt)}{2} \left[\exp(y\sqrt{P-b}) \operatorname{erfc} \left(\frac{y}{2\sqrt{t}} + \sqrt{(P-b)t} \right) + \exp(-y\sqrt{P-b}) \operatorname{erfc} \left(\frac{y}{2\sqrt{t}} - \sqrt{(P-b)t} \right) \right]$$

$$B_3 = \frac{\exp(-ct)}{2} \left[\exp(y\sqrt{P-c}) \operatorname{erfc} \left(\frac{y}{2\sqrt{t}} + \sqrt{(P-c)t} \right) + \exp(-y\sqrt{P-c}) \operatorname{erfc} \left(\frac{y}{2\sqrt{t}} - \sqrt{(P-c)t} \right) \right]$$

$$B_4 = \frac{1}{2} \left[\exp(y\sqrt{R}) \operatorname{erfc} \left(\frac{y\sqrt{Pr}}{2\sqrt{t}} + \sqrt{\frac{Rt}{Pr}} \right) + \exp(-y\sqrt{R}) \operatorname{erfc} \left(\frac{y\sqrt{Pr}}{2\sqrt{t}} - \sqrt{\frac{Rt}{Pr}} \right) \right]$$

$$B_5 = \frac{\exp(-bt)}{2} \left[\exp(y\sqrt{R-bPr}) \operatorname{erfc} \left(\frac{y\sqrt{Pr}}{2\sqrt{t}} + \sqrt{\frac{Rt}{Pr} - bt} \right) + \exp(-y\sqrt{R-bPr}) \operatorname{erfc} \left(\frac{y\sqrt{Pr}}{2\sqrt{t}} - \sqrt{\frac{Rt}{Pr} - bt} \right) \right]$$

$$B_6 = \frac{1}{2} \left[\exp(y\sqrt{kSc}) \operatorname{erfc} \left(\frac{y\sqrt{Sc}}{2\sqrt{t}} + \sqrt{kt} \right) + \exp(-y\sqrt{kSc}) \operatorname{erfc} \left(\frac{y\sqrt{Sc}}{2\sqrt{t}} - \sqrt{kt} \right) \right]$$

$$B_7 = \frac{\exp(-ct)}{2} \left[\exp(y\sqrt{(k-c)Sc}) \operatorname{erfc} \left(\frac{y\sqrt{Sc}}{2\sqrt{t}} + \sqrt{(k-c)t} \right) + \exp(-y\sqrt{(k-c)Sc}) \operatorname{erfc} \left(\frac{y\sqrt{Sc}}{2\sqrt{t}} - \sqrt{(k-c)t} \right) \right]$$

$$B_8 = \left(\frac{t}{2} + \frac{y}{4\sqrt{P-b}} \right) \exp(y\sqrt{P-b}) \operatorname{erfc} \left(\frac{y}{2\sqrt{t}} + \sqrt{(P-b)t} \right) + \left(\frac{t}{2} - \frac{y}{4\sqrt{P-b}} \right) \exp(-y\sqrt{P-b}) \operatorname{erfc} \left(\frac{y}{2\sqrt{t}} - \sqrt{(P-b)t} \right)$$

$$B_9 = \left(\frac{t}{2} + \frac{y}{4\sqrt{P-c}} \right) \exp(y\sqrt{P-c}) \operatorname{erfc} \left(\frac{y}{2\sqrt{t}} + \sqrt{(P-c)t} \right) + \left(\frac{t}{2} - \frac{y}{4\sqrt{P-c}} \right) \exp(-y\sqrt{P-c}) \operatorname{erfc} \left(\frac{y}{2\sqrt{t}} - \sqrt{(P-c)t} \right)$$

$$B_{10} = \left(\frac{t}{2} + \frac{yPr}{4\sqrt{R-bPr}} \right) \exp(y\sqrt{R-bPr}) \operatorname{erfc} \left(\frac{y\sqrt{Pr}}{2\sqrt{t}} + \sqrt{\frac{Rt}{Pr} - bt} \right) + \left(\frac{t}{2} - \frac{yPr}{4\sqrt{R-bPr}} \right) \exp(-y\sqrt{R-bPr}) \operatorname{erfc} \left(\frac{y\sqrt{Pr}}{2\sqrt{t}} - \sqrt{\frac{Rt}{Pr} - bt} \right)$$

$$B_{11} = \left(\frac{t}{2} + \frac{y\sqrt{Sc}}{4\sqrt{k-c}} \right) \exp(y\sqrt{(k-c)Sc}) \operatorname{erfc} \left(\frac{y\sqrt{Sc}}{2\sqrt{t}} + \sqrt{(k-c)t} \right) + \left(\frac{t}{2} - \frac{y\sqrt{Sc}}{4\sqrt{k-c}} \right) \exp(-y\sqrt{(k-c)Sc}) \operatorname{erfc} \left(\frac{y\sqrt{Sc}}{2\sqrt{t}} - \sqrt{(k-c)t} \right)$$

$$B_{12} = \left(\frac{y^3 - 2t}{4t^2 \sqrt{\pi t}} \right) \exp \left[- \left(\frac{y^2}{4t} + Pt \right) \right], \quad B_{13} = \frac{\exp \left[- \left(\frac{y^2}{4t} + Pt \right) \right]}{\sqrt{\pi t}}$$

$$B_{14} = \frac{\exp(-bt)\sqrt{P-b}}{2} \left[\exp(-y\sqrt{P-b}) \operatorname{erfc} \left(\frac{y}{2\sqrt{t}} - \sqrt{(P-b)t} \right) - \exp(y\sqrt{P-b}) \operatorname{erfc} \left(\frac{y}{2\sqrt{t}} + \sqrt{(P-b)t} \right) \right]$$

$$B_{15} = \frac{\exp(-ct)\sqrt{P-c}}{2} \left[\exp(-y\sqrt{P-c}) \operatorname{erfc} \left(\frac{y}{2\sqrt{t}} - \sqrt{(P-c)t} \right) - \exp(y\sqrt{P-c}) \operatorname{erfc} \left(\frac{y}{2\sqrt{t}} + \sqrt{(P-c)t} \right) \right]$$

$$P = M + \frac{1}{K}, \quad b = \frac{R-P}{Pr-1}, \quad c = \frac{kSc-P}{Sc-1}$$

2.2 The rate of heat transfer

From temperature field, now we study the rate of heat transfer which is given in non-dimensional form as:

$$Nu = - \left[\frac{d\theta}{dy} \right]_{y=0} \quad (16)$$

From equations (13) and (16), we get

$$Nu = \sqrt{\frac{Pr}{\pi t}} \exp \left(- \frac{Rt}{Pr} \right) + \sqrt{R} \operatorname{erf} \left(\sqrt{\frac{Rt}{Pr}} \right) \quad (17)$$

The rate of mass transfer

From concentration field, now we study the rate of mass transfer which is given in non-dimensional form

$$Sh = - \left(\frac{dC}{dy} \right)_{y=0} \quad (18)$$

From equations (14) and (18), we get

$$Sh = \sqrt{\frac{Sc}{\pi t}} \exp(-kt) + \sqrt{kSc} \operatorname{erf}(\sqrt{kt}) \quad (19)$$

III. RESULTS AND DISCUSSION

In Figures from (2) to (23) for the case of cooling ($G_r > 0, G_m > 0$) and heating ($G_r < 0, G_m < 0$) for $M = 1$, $S = 0.5$, $G_m = 5$, $G_r = 10$, $K = 0.5$, $k = 5$, $Pr = 0.1$, $Sc = 0.78$, $R = 6$, $t = 0.4$. Figures 1 and 2 reveal that the velocity variations with viscoelastic parameter in the cases of cooling and heating of the plate at time $t = 0.4$. It is observed that the velocity increases while increasing elasticity of the fluid, velocity up to the range $0 < y < 0.5$ then decreases in case of cooling of the plate. The opposite reaction is found in the case of heating of the plate, finally takes asymptotic values at $y = 2.5$ for both the cases. It may be concluded that the energy due to elastic property of the fluid increases the velocity and then gets dissipated. The influence of the thermal radiation parameter on the velocity profile is shown in Figures 3 and 4 for both cooling and heating cases respectively. Figure 3 shows that the radiation parameter tends to reduce the fluid velocity for ($G_r > 0, G_m > 0$) and the reverse effect will be found for ($G_r < 0, G_m < 0$) in figure 4. This is because those large values of R correspond to an increased dominance of conduction over absorption radiation, thereby increasing the buoyancy force and thickness of the momentum boundary layer. The effect of the magnetic field parameter M is shown in Figures 5 and 6 in the case of cooling and as well as heating of the plate. It is observed that the velocity of the fluid decreases with the increase of the magnetic parameter values for cooling of the plate at time 0.4. As expected, the velocity decreases with an increase in the magnetic parameter. It is because the application of the transverse magnetic field will result in a resistive type force (Lorentz force) similar to the drag force which tends to resist the

fluid flow and thus reducing its velocity. Also, the boundary layer thickness decreases with an increase in the magnetic parameter. It is also seen that the velocity profiles decrease with the increase of the magnetic effect indicating that the magnetic field tends to retard the motion of the fluid. The magnetic field may control the flow characteristics. The reverse phenomenon is found in the case of heating of the plate. Figures 7 and 8 show the velocity profiles for different Prandtl numbers corresponding to different substances for cooling and heating of the plate: $(Pr = 0.025)$ mercury, $(Pr = 0.05)$ lithium and $(Pr = 0.1)$. It is identified that the velocity decreases with the increase in the Prandtl number for cooling of the plate at time 0.4. It is evident from the figures that the thermal boundary-layer thickness is greater for fluids with small Prandtl number. The reason is that smaller values of Pr are equivalent to an increasing thermal conductivity, and therefore such fluid heat is able to diffuse away from the heated surface more rapidly than for fluids with higher Pr values. But the reverse effect is observed in the case of cooling of the plate. Figures 9 and 10 represent that the velocity profiles for different values of t (time) in cases of cooling and heating of the plate respectively. From these figures, in the case of cooling, the velocity is found to increase with an increase in time t . But the reverse effect is observed in the case of heated plate. The effect of the chemical reaction parameter (k) has shown in Figures 11 and 12 in the case cooling and heating of the plate. As expected, the presence of the chemical reaction significantly affects both profiles. It should be mentioned that the case studied relates to a destructive chemical reaction. In fact, as the chemical reaction parameter increases, a considerable reduction in the velocity occurs, and the presence of the peak indicates that the maximum velocity takes place in the fluid body close to the surface, but not at the surface itself. It is evident that an increase in this parameter significantly alters the concentration of boundary-layer thickness but does not change the momentum one. It is very clear from Figure 13 that an increase in porosity parameter leads to enhance the velocity profiles for cooling of the plate at time $t = 0.4$, because it reduces the drag force. But the reverse effect is observed from Figure 14 in the case of heating of the plate. Figures 15 and 16 display the effects of Sc (Schmidt number) on the velocity field for the cases of cooling and heating of the plate at $t = 0.4$ respectively. From these figures, in cooling case, it is found that the velocity increases with an increase in Sc . But the reverse effect is found in heating case. The temperature of the flow field is mainly affected by the flow parameters, namely, radiation parameter and time. From Figures (17) and (18), it is observed when radiation parameter R increases, the temperature of the flow field decreases at all the points in flow region. Hence, it is observed that the temperature for conducting air ($Pr = 0.71$) is higher than that of water ($Pr = 7.0$) this is because of the fact that thermal conductivity of the fluid decreases with increasing values of Pr resulting decrease in thermal boundary layer thickness. Therefore, using radiation we can control temperature distribution and flow transport. It is also seen that temperature increases as time increases, and it leads to zero as it moves away from the plate. The effect of concentration profiles for different values of chemical reaction parameter, Schmidt number and time are illustrated in Figures (19) and (20) and it is found that the concentration decreases as chemical reaction parameter or Schmidt number increases while it increases with increasing values of time. It is obviously seen that from Figure (21) the rate of heat transfer is measured in terms of Nusselt number found increasing to increase with an increase in R for both water at 200C ($Pr = 7.0$) and conducting air ($Pr = 0.71$). It is also observed that the rate of heat transfer in water is more than in air, it is due to the fact that the smaller values of Pr are equivalent to increasing the thermal conductivities and therefore heat is able to diffuse more away from surface more rapidly than greater values of Pr , hence there is a reduction in heat transfer coefficient. Finally, from Figure (22) it is noticed that Sherwood number increases as Schmidt parameter or chemical reaction parameter increases.

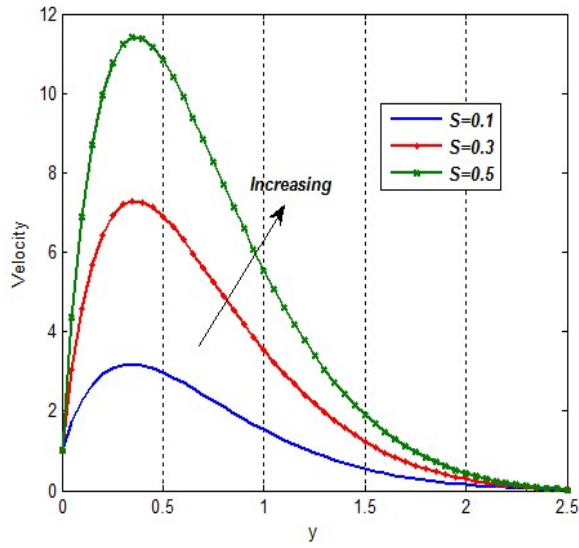


Fig.1 Velocity profile for different values of S

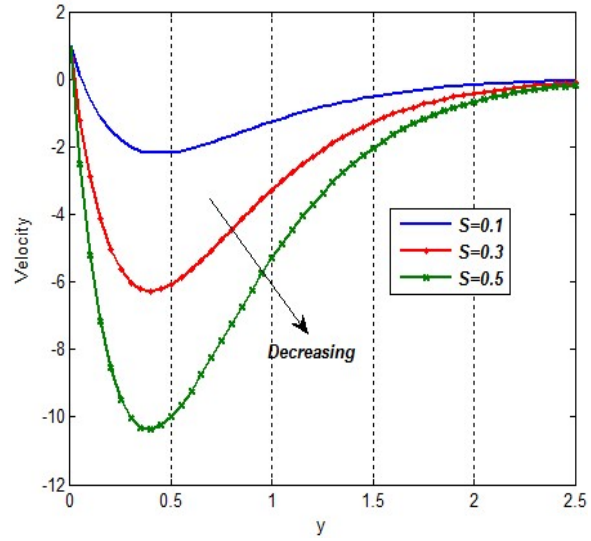


Fig.2 Velocity profile for different values of S

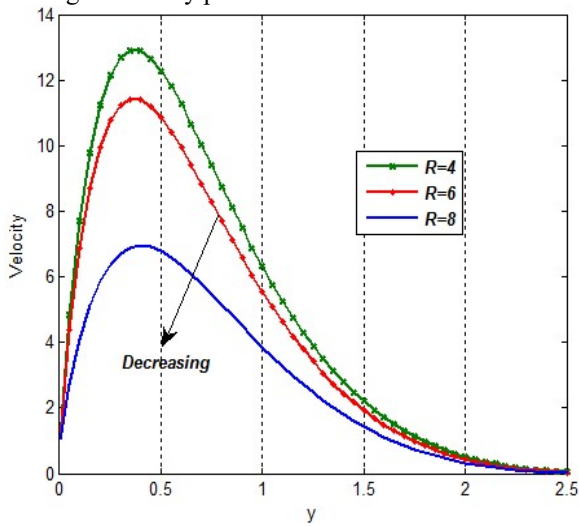


Fig.3. Velocity profile for different values of R

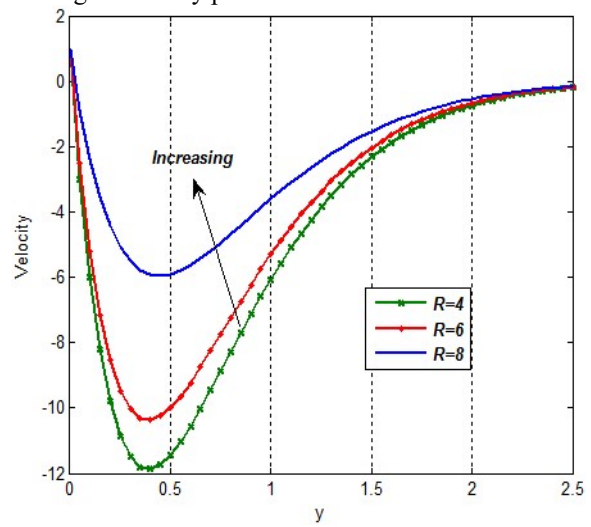


Fig.4 Velocity profile for different values of R

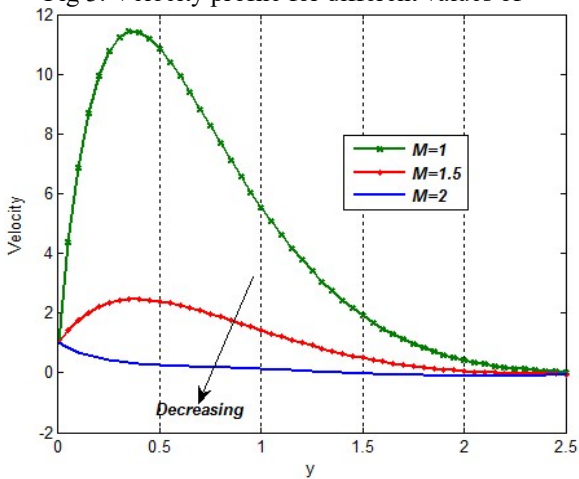


Fig.5 Velocity profile for different values of M

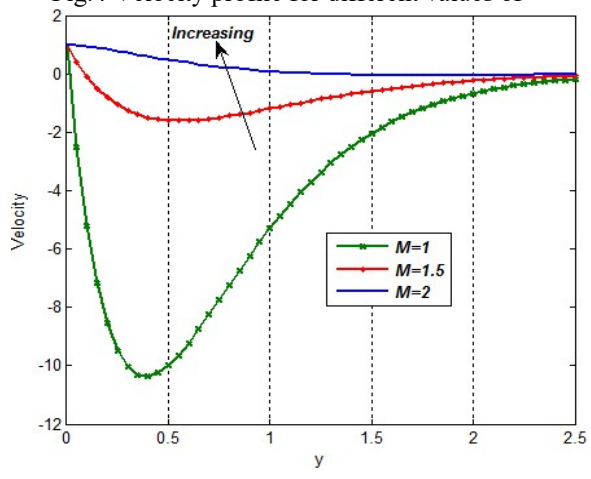


Fig.6 Velocity profile for different values of M

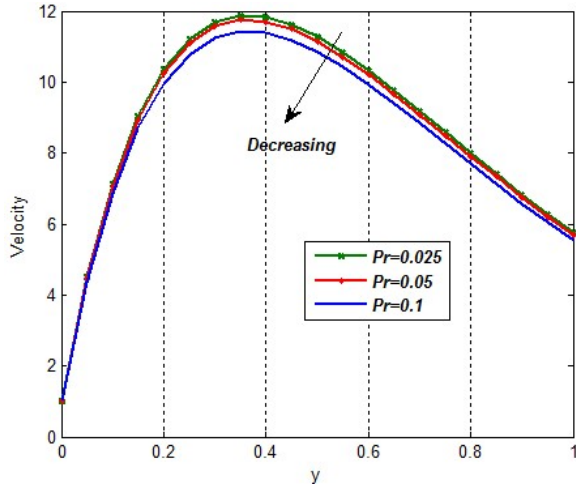


Fig.7 Velocity profile for different values of Pr

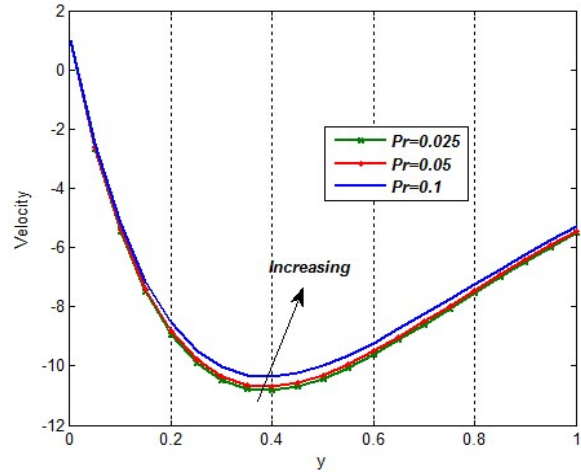


Fig.8 Velocity profile for different values of Pr

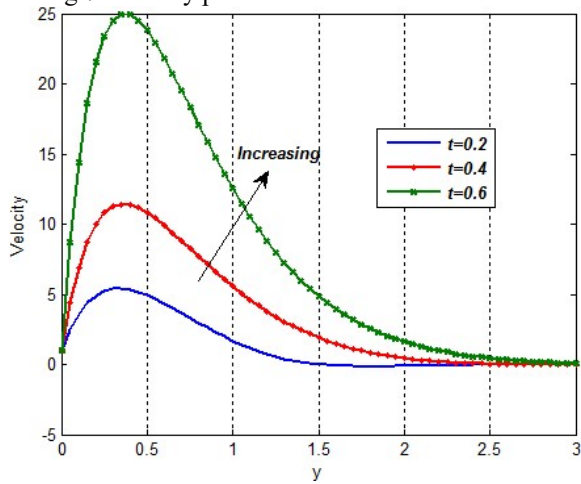


Fig.9 Velocity profile for different values of t

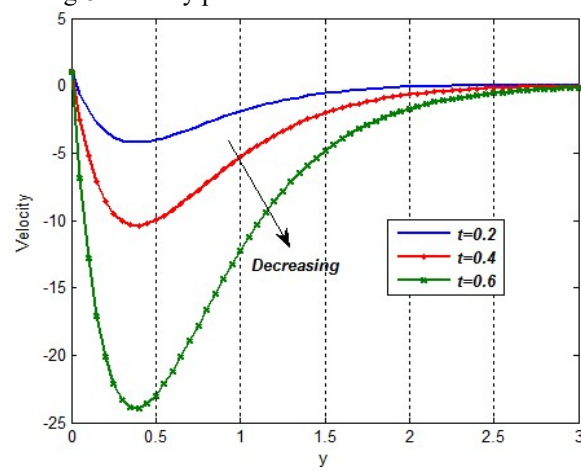


Fig.10 Velocity profile for different values of t

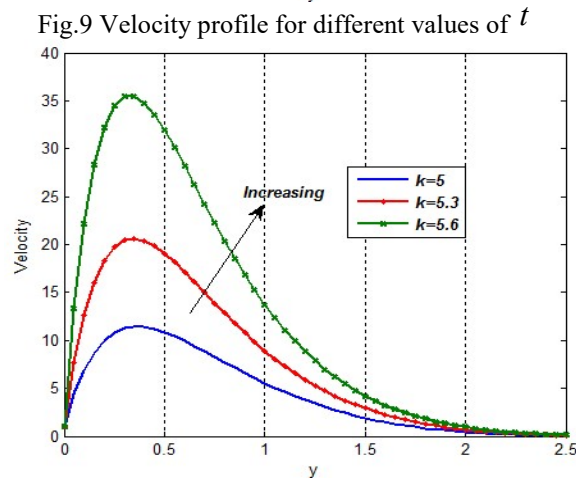


Fig.11 Velocity profile for different values of k

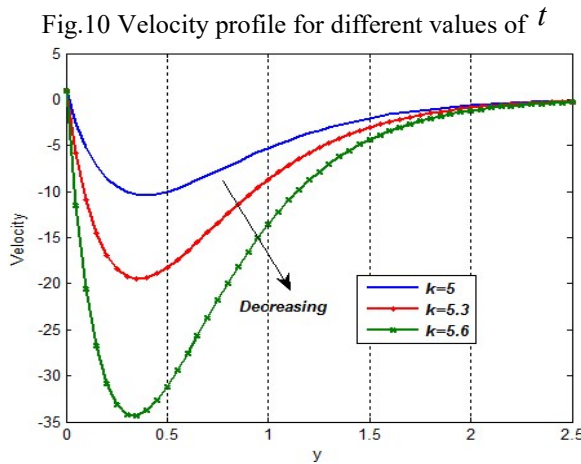


Fig.12 Velocity profile for different values of k

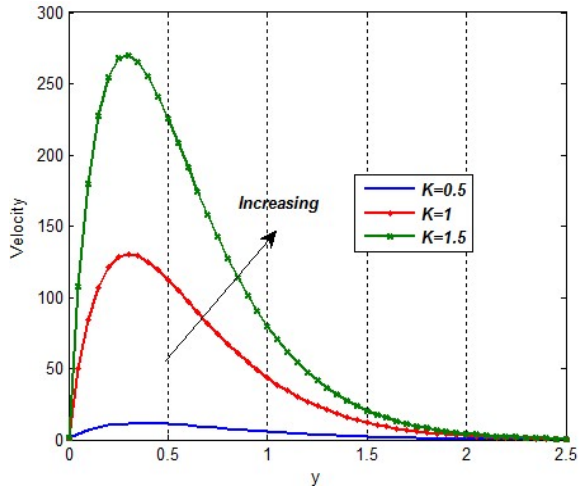


Fig.13 Velocity profile for different values of K

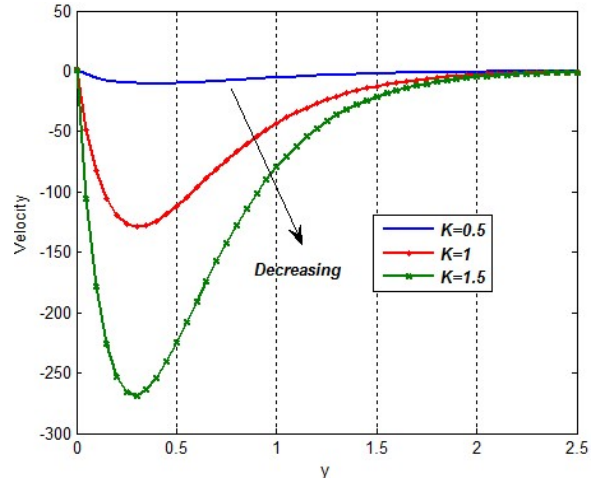


Fig.14 Velocity profile for different values of K

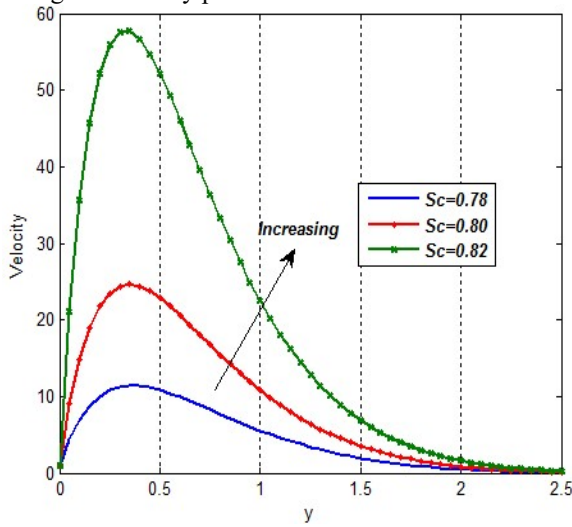


Fig.15 Velocity profile for different values of Sc

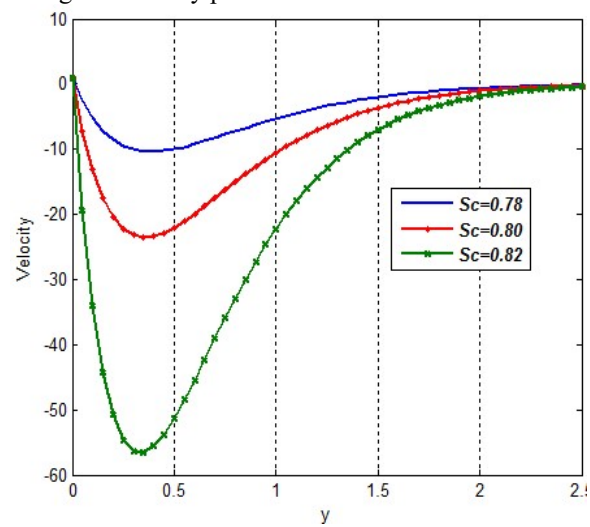


Fig.16 Velocity profile for different values of Sc

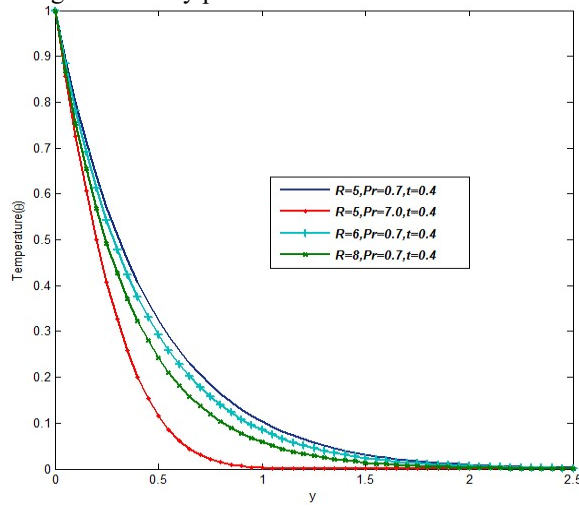


Fig.17 Temperature profile for R & Pr

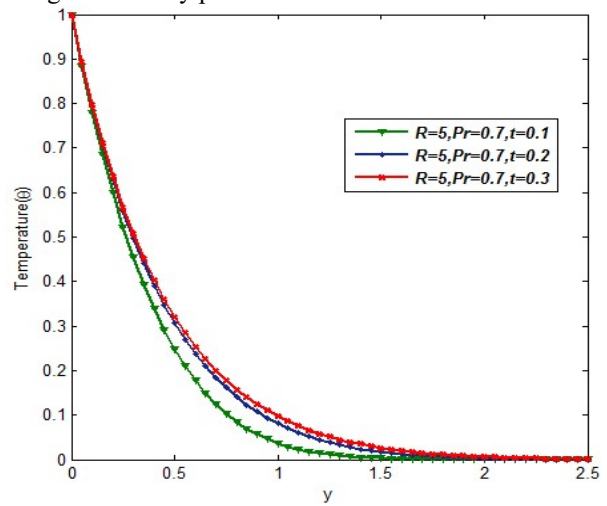


Fig.18 Temperature profile for t

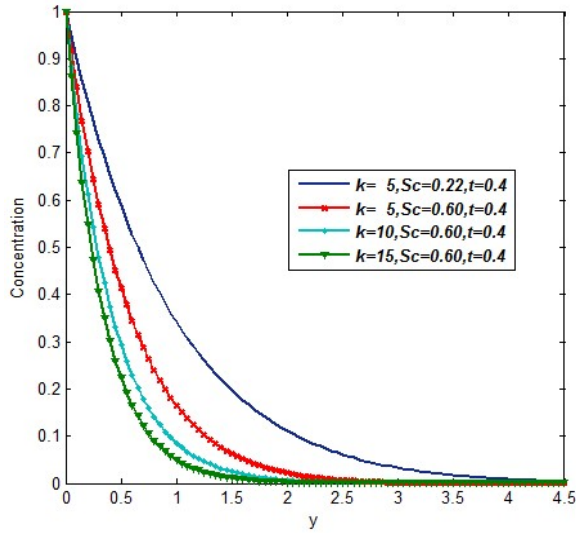


Fig.19 Concentration profile for k & Sc

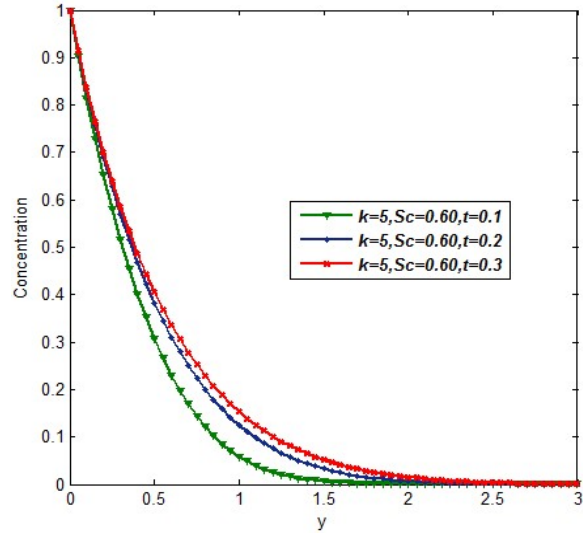


Fig.20 Concentration profile for t

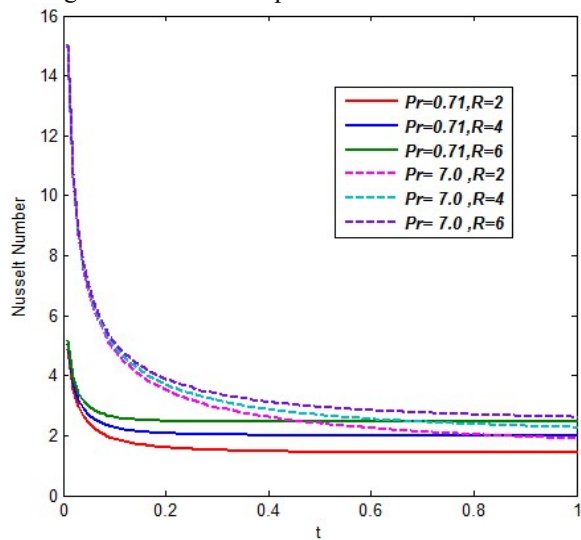


Fig.21 Nusselt Number

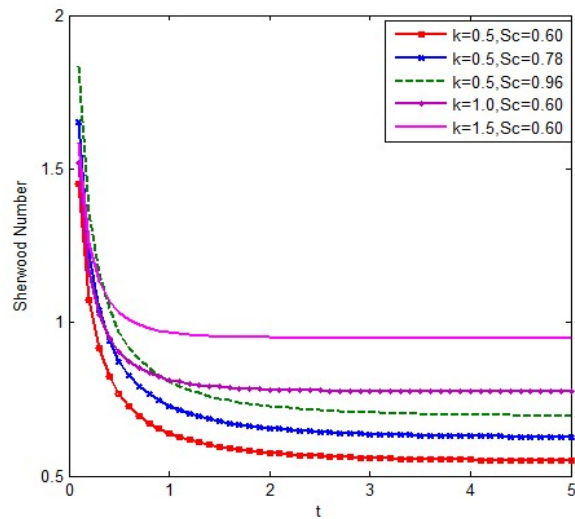


Fig.22 Sherwood Number

IV. CONCLUSION

A theoretical investigation is performed on unsteady free convective chemically reacting, MHD visco-elastic fluid (Walter's liquid-B model) flow past an infinite vertical plate with uniform temperature and concentration in the presence of transverse magnetic field through porous medium. Exact solutions are obtained by employing the Laplace transform technique and in response the following conclusions are made:

The fluid velocity increases with increasing parameters viscoelastic, porosity, chemical reaction, Schmidt number and time for cooling of the plate, whereas its decreases in heating of the plate.

The velocity of the fluid decreases with increasing Prandtl number, magnetic field parameter and radiation parameter in case of cooling of the plate, whereas the reverse effect found in the case of heating of the plate.

The fluid temperature decreases with increasing values of R and Pr , but when time increases the temperature is increase.

The fluid concentration decreases with increase k & Sc , the reverse effect for increasing time.

When radiation Prandtl number is increased the rate of heat transfer also increases and The Sherwood number is increasing with the increase Sc & k .

V. REFERENCES

- [1] G. G. Stokes, Trans. Cambr. Phil. Soc. 9, 1851, pp. 8.
- [2] K. Walters, J. Mech. 1, 1962, pp. 479.
- [3] D.W. Beard and K. Walters, Elastico-viscous boundary layer flow in two dimensional flows near a stagnation point. Proc. Cambr. Phil. Soc. 60, 1964, pp. 667-674.
- [4] V. G. Kubair and D.C.T. Pei, Combined laminar free and forced convection heat transfer to non-Newtonian fluids, Int. J. Heat mass Transfer, 11, 1968, pp. 855-869.
- [5] L. Teipel, The impulsive motion of a flat plate in a viscoelastic fluid. Acta Mechanica, 39, 1981, pp. 277-279.
- [6] A. R. Bestman, Numerical studies of laminar convection of a radiating Non-Newtonian fluid in a vertical porous channel. Number Methods Thermal Problem, 3, 1983, pp. 574-583.
- [7] R. Bestman, Free convection heat transfer to steady radiating Non-Newtonian MHD flow past a vertical porous plate. Int. J. Numerical Methods in Engineering, 21, 1985, pp. 899-908.
- [8] K. Singh, Finite difference analysis of MHD free-convection flow past an accelerated vertical porous plate, Astrophysics and Space Science, 94, 1983, pp. 395-400.
- [9] S. Singh, MHD flow of an elastic-viscous fluid past an impulsively started vertical plate, Ganit (Bangladesh Math Soc.), 1, 1984, pp. 35-39.
- [10] S. Dandpath and A. S. Gupta, The flow and heat transfer in a visco-elastic fluid over a stretching shell. Int. J. Non-Linear Mech. 24(3), 1989, pp. 215-219.
- [11] K. R. Choubey and R. R., Yadav, Magneto hydrodynamic flow of a Non-Newtonian fluid past a porous plate. Astrophysics and Space Science, 115, 1985, pp. 345-351.
- [12] K. Jha, MHD free-convection and mass transfer flow of an elasto-viscous fluid, Astrophysics and Space Science, 185 (1), 129, 1991, pp. - 135.
- [13] N. K. Samria, R. Prasad and M. U. S. Reddy, MHD free-convection flow of a visco-elastic fluid past an infinite vertical plate. Astrophysics and Space Science, 181, 1991, pp. 135-145.
- [14] M. K. Chowdhury and M. N. Islam, MHD free convection flow of visco-elastic fluid past an infinite vertical porous plate, Heat and Mass transfer. 36 (5), 2000, pp. 439 – 447.
- [15] Vijaya Kumar, A.G., Kumaresan, E., Varma, S.V.K.: An exact analysis of unsteady MHD free convective chemically reacting elasto-viscous fluid flow past an impulsively started infinite vertical plate through porous medium in the presence of radiation absorption. Int. J. Appl. Comput. Math. 3, 1–18 (2016)
- [16] Kumaresan, E., Vijaya Kumar, A.G., Prakash, J.: Exact Solution of Unsteady MHD Free Convective Chemically Reacting Visco-Elastic Fluid Flow Past a Moving Vertical Plate Through Porous Medium. Int. J. Appl. Comput. Math. (2017)
- [17] S. K. Khan and I. Pop, Unsteady free convective viscoelastic boundary layer flow past a vertical porous plate with internal heat generation/absorption, International Journal of Fluid Mechanics Research, 33 (6), 2006, pp. 500 – 522.
- [18] M. Hameed and Nadeem, Unsteady MHD flow of a Non-Newtonian fluid on a porous plate, J. Math. Anal. 325, 2007, pp. 724-733.
- [19] R. A. Damesh and B. A. Shannak, Visco-elastic fluid flow past an infinite vertical porous plate in the presence of first order chemical reaction. Appl. Math. Mech. 31, 2010, pp. 955-962.
- [20] T. M. N. Eldabe, S. N. Sallam and M. Y. Abou-Zeid, Numerical study of viscous dissipation effect on free convection heat and mass transfer of MHD non-Newtonian fluid flow through a porous medium, Journal of the Egyptian Mathematical Society, 20 (2), 2012, pp. 139-151

NOMECLATURE

A	Constant
y'	Coordinate axis normal to the plate
y	Dimensionless coordinate axis normal to the plate
u	Dimensionless velocity
u'	Velocity of the fluid in the x' - direction
u_0	Velocity of the plate
g	Acceleration due to gravity
M	Magnetic field parameter
B_0	External magnetic field
G_r	Thermal Grashof number
G_m	Mass Grashof number
K'	Dimensional permeability parameter
K	Dimensionless permeability parameter
K_0	Dimensional Walter's- B model parameter
S	Visco-elastic parameter
T_∞'	Temperature of the fluid far away from the plate
T_w'	Temperature of the plate

T'	Temperature of the fluid near the plate
κ	Thermal conductivity of the fluid
θ	Dimensionless temperature
R	Radiation parameter
Pr	Prandtl number
C_{∞}'	Concentration in the fluid far away from the plate
C_w'	Concentration near of the plate
C	Dimensionless concentration
C'	Species concentration in the fluid
C_p	Specific heat at constant pressure
C_s	Concentration susceptibility
D_m	Coefficient of mass diffusivity
D	Chemical molecular diffusivity
Sc	Schmidt number
K_r	Dimensional chemically reaction parameter
k	Dimensionless chemically reaction parameter
t'	Time
t	Dimensional time
μ	Coefficient of viscosity
$erfc$	Complementary error function
erf	Error function
ρ	Density of the fluid
σ	Electric conductivity
ν	Kinematic viscosity
α	Thermal diffusivity
β^*	Volumetric coefficient of expansion with concentration
β	Volumetric coefficient of thermal expansion
W	Conditions on the wall
∞	Free stream conditions